CO poisoning of ethylene hydrogenation over Pt catalysts: a comparison of Pt(111) single crystal and Pt nanoparticle activities

Jeff Grunes, Ji Zhu, Minchul Yang, and Gabor A. Somorjai *

Department of Chemistry and Division of Materials Science, Lawrence Berkeley National Laboratory, University of California, Berkeley, CA 94720, USA

Received 28 October 2002; accepted 16 December 2002

The ethylene hydrogenation reaction was studied on two platinum model catalyst systems in the presence of carbon monoxide to examine poisoning effects. The catalysts were a Pt(111) single crystal and lithographically fabricated platinum nanoparticles deposited on alumina. Gas chromatographic results for Pt(111) show that CO adsorption reduces the turnover rate from 10^1 to 10^{-2} molecules/Pt site/s at 413 K, and the activation energy for hydrogenation on the poisoned surface becomes 20.2 ± 0.1 kcal/mol. The activation energy for ethylene hydrogenation over Pt(111) in the absence of CO is 10.8 kcal/mol. The Pt nanoparticle system shows the same rate for the reaction as over Pt(111) in the absence of CO. When CO is adsorbed on the Pt nanoparticle array, the rate of the reaction is reduced from 10^2 to 10^0 nmol/s at 413 K. However, the activation energy remains largely unchanged. The Pt nanoparticles show an apparent activation energy for ethylene hydrogenation of 10.2 ± 0.2 kcal/mol in the absence of CO and 11.4 ± 0.6 kcal/mol on the CO-poisoned nanoparticle array. This is the first observation of a significant difference in catalytic behavior between Pt(111) and the Pt nanoparticle arrays. It is proposed that the active sites at the oxide–metal interface are responsible for the difference in activation energies for the hydrogenation reaction over the two model platinum catalysts.

KEY WORDS: CO poisoning; ethylene hydrogenation over Pt; Pt/Al_2O_3 nanoparticles.

1. Introduction

Catalytic reactions carried out on single crystal surfaces have yielded extensive information on the atomic and molecular features that control turnover rates, and they continue to serve as important model catalysts. However, most industrial catalysts consist of highly dispersed metal particles supported on an oxide surface. In order to construct model systems that have metals in nanoparticle form as well as oxide supports, electron beam lithography (EBL) has been used to control precisely the architecture of our model catalyst. Experiments since the 1970s have identified the important factors that govern catalysis, such as metal catalyst surface structure [1–5], metal–oxide interfaces [6–9], and the diffusion of surface species between the oxide and the metal [10]. A structure-sensitive reaction will show a dependence on the specific crystallographic face of a metal or the metal particle size [11]. The advantages of EBL include control over and uniformity in metal particle size (10–100 Å in diameter) and particle periodicity. The technique itself is not dependent on the materials, so a variety of metals can be coupled with a range of supports.

A catalyst must remain active for a number of years in order to be successful. Deactivation is therefore a prime concern when developing industrial catalysts. During a reaction, the catalyst surface can be covered by reactants, intermediates, products, or unwanted species. The species can block the active sites of the catalyst, thus changing the properties of the catalyst over time [12]. Infrared absorption spectra of adsorbed carbon monoxide on several transition metals exhibit different spectral features when the CO adsorbs at different sites on the metal surface [13–18]. Carbon monoxide is therefore often used as a probe molecule to determine the availability of adsorption sites during a catalytic reaction [19]. It is well known that CO adsorption can poison hydrocarbon reactions. In this work, we examined the ethylene hydrogenation reaction over Pt model catalysts in the presence and absence of CO and proposed mechanisms that govern the CO-poisoned reaction.

2. Experimental

2.1. Pt(111) single crystal model catalysts: characterization and reaction rate studies

The experimental apparatus consists of an ultra-high vacuum (UHV) chamber coupled with a high-pressure (HP) reaction cell. The catalyst was cleaned and characterized in the UHV chamber, and the HP reaction cell was used to monitor the catalytic reaction via gas chromatography (GC). A detailed description of the experimental set-up can be found elsewhere [20].

* To whom correspondence should be addressed.
E-mail: somorjai@cchem.berkeley.edu

1011-372X/03/0300-0157/0

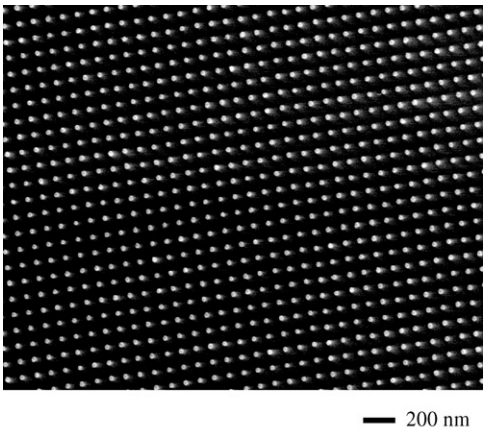

Figure 1. Field emission scanning electron microscopy (FESEM) image of the platinum nanoparticle array showing a particle diameter of 28 ± 2 nm and a periodicity of 100 ± 2 nm.

The Pt(111) single crystal was cleaned in UHV by cycles of Ar^+ sputtering, O_2 treatment, and annealing [21]. After the single crystal had been cleaned, the HP reaction cell was closed and the gas mixture was introduced. The reaction gas mixture for the Pt(111) single crystal included 10 Torr C_2H_4, 1 Torr CO, 100 Torr H_2, and Ar make-up gas to bring the total gas pressure to 760 Torr. The reaction was then monitored over time for product accumulation by GC.

2.2. Pt nanoparticles on alumina: fabrication, characterization, and reaction rate studies

The details of the EBL fabrication process for the Pt nanoparticle array model catalyst have been reported elsewhere [22,23]. Briefly, a highly collimated electron beam is used to expose a thin layer of poly(methyl methacrylate) (PMMA), which is spin-coated on an Si(100) wafer that is coated with 15 nm of alumina (Al_2O_3). The electron irradiation decomposes the polymer backbone, making it possible to dissolve the exposed polymer in a developing solution. A 15 nm thick Pt film was deposited on the surface by electron beam evaporation. The remaining PMMA was removed with acetone and ultrasonication. The alumina-supported Pt nanoparticle array model catalyst has a 100 ± 2 nm interparticle spacing with particle diameters of 28 ± 2 nm (figure 1). The sample was characterized by field emission scanning electron microscopy (FESEM), atomic force microscopy (AFM), and X-ray photoelectron spectroscopy (XPS).

The Pt nanoparticle system was cleaned with NO_2, followed by dosing the sample with CO and flashing the temperature to 573 K. This removes the major impurities on the surface, such as oxygen and carbon. This procedure has been established to be safe and effective for cleaning the Pt nanoparticles [24]. The catalysis study was performed in a similar UHV chamber with an HP reaction cell. The details of this experimental set-up are described elsewhere [24]. The reaction gases were pre-mixed in a gas manifold before being introduced into the HP reaction cell. The reaction gas mixture consisted of 10 Torr C_2H_4, 0.3 Torr CO, 100 Torr H_2, and Ne make-up gas to bring the total gas pressure to 760 Torr. The products were analyzed by GC.

3. Results and discussion

3.1. Ethylene hydrogenation reaction rate studies on Pt(111): effects of temperature

The poisoning effects of CO for the ethylene hydrogenation reaction over Pt(111) were investigated from 400 to 523 K. Arrhenius plots of the initial turnover frequency (TOF) as a function of $1/T$ for ethylene hydrogenation with (●) and without (■) CO over Pt(111) are shown in figure 2. Turnover frequency (TOF) is defined as the number of ethane molecules generated per Pt surface atom per second. When CO is adsorbed, the TOF is reduced by 2–3 orders of magnitude, depending on the temperature. At 413 K, the reaction rate for ethylene hydrogenation over the Pt(111) single crystal in the presence of CO is reduced from 10^1 to 10^{-2} molecules/Pt site/s; at 473 K, the reaction rate for ethylene hydrogenation over the Pt(111) single crystal in the presence of CO is reduced from 10^2 to 10^0 molecules/Pt site/s. Activation energies obtained from the slopes in figure 2 for ethylene hydrogenation over the Pt(111) single crystal in the presence and absence of CO are 20.2 ± 0.1 and 9.6 ± 0.4 kcal/mol, respectively. The measured activation energy for ethylene hydrogenation over Pt(111) in the absence of CO is consistent with previous studies, which reported an activation energy of 10.8 kcal/mol [25].

The measured activation energy for ethylene hydrogenation on Pt(111) in the presence of 1 Torr CO, 20.2 ± 0.1 kcal/mol, is close in value to the desorption energy of CO on Pt(111). Carbon monoxide is known to form an incommensurate hexagonal overlayer on the surface, with a coverage of 0.60 ML, when the species is present in the mTorr range and above [26]. At this coverage, the heat of adsorption of CO is 22 ± 4 kcal/mol [27]. The proximity of this value with the ethylene hydrogenation activation energy suggests a possible correlation that needs further investigation.

3.2. Ethylene hydrogenation reaction rate studies on Pt nanoparticles supported on alumina: effects of temperature

The ethylene hydrogenation reaction over the Pt nanoparticles, with and without CO, was studied over the range 313 to 523 K. The activity of the Pt nanoparticles

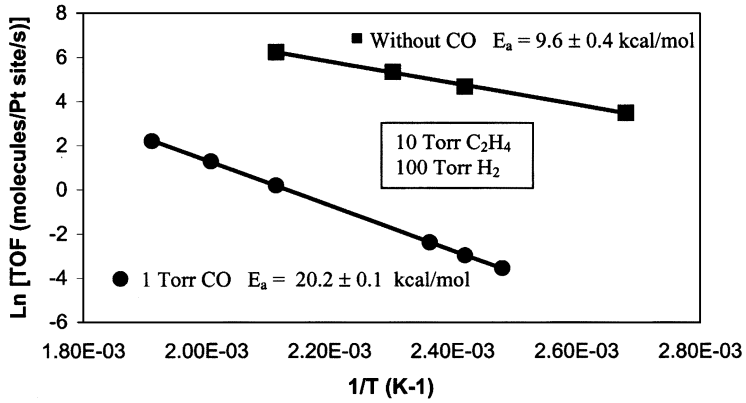

Figure 2. Logarithmic plots of turnover frequency (TOF) *versus* $1/T$ for ethylene hydrogenation with (●) and without (■) CO over Pt(111). The activation energies obtained from the slopes are 20.2 ± 0.1 and 9.6 ± 0.4 kcal/mol with and without CO present, respectively.

with 0.3 Torr CO is less than 5% of the activity without CO at the same temperature, as defined as the percent conversion of ethylene to ethane molecules. At 413 K, the reaction rate for ethylene hydrogenation over the Pt nanoparticle array model catalyst in the presence of CO is reduced from 10^2 to 10^0 nmol/s. The reaction without CO was investigated from 313 to 423 K. Reactions conducted above 423 K proceeded too quickly to permit an accurate measurement of the reaction rate. Conversely, because the catalytic activity of the Pt nanoparticles was greatly inhibited in the presence of CO, the poisoning reaction was studied from 373 to 523 K in order to obtain results that were distinguishable from the background reaction in the experimental timeframe.

Arrhenius plots for the ethylene hydrogenation reaction with (◆) and without (□) CO over the Pt nanoparticle array model catalyst are shown in figure 3. The graph shows that the activation energy for ethylene hydrogenation without CO (10.2 ± 0.2 kcal/mol) is virtually identical with that for the reaction with 0.3 Torr CO (11.4 ± 0.6 kcal/mol). The same effects on the ethylene hydrogenation reaction over the Pt nanoparticle array model catalyst are seen for reactions poisoned with either 0.6 or 0.3 Torr CO. The reaction rate at 413 K is reduced by two orders of magnitude and the activation energy remains the same.

The activation energy difference between the Pt(111) single crystal and the Pt nanoparticle array model catalyst for a reaction poisoned by CO is significant. Because the activation energy is largely unchanged for the nanoparticle array in the presence of CO, concentrations of Pt sites are still available for ethylene hydrogenation. It is known that CO hydrogenation is enhanced at oxide–metal interfaces [28]. Therefore, these interface sites could remain free of CO in order to continue

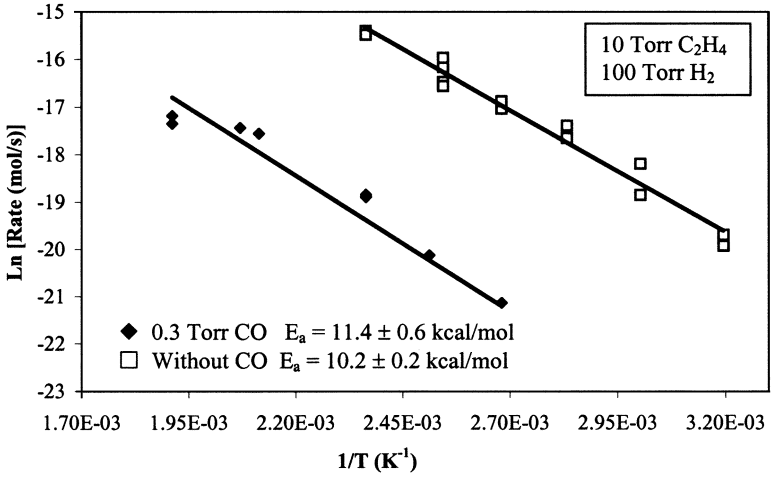

Figure 3. Arrhenius plots of the rate of ethylene hydrogenation *versus* $1/T$ on platinum nanoparticle arrays with (◆) and without (□) CO. The activation energies obtained from the slopes are 11.4 ± 0.6 and 10.2 ± 0.2 kcal/mol with and without CO present, respectively.

hydrogenating the ethylene. With increasing CO pressure, fewer CO free sites are available. On the single crystal, all available Pt sites are poisoned by CO. In this case, CO molecules must desorb in order for hydrogenation to take place on the metal surface. This helps explain why the activation energy for ethylene hydrogenation on Pt(111) in the presence of CO is equal to that of the heat of desorption of carbon monoxide.

The main difference between the Pt(111) single crystal and the Pt nanoparticle array is the oxide–metal interface. Hydrogenation can take place at either of two sites. First, there are metal sites that exist on both model catalyst systems and are prone to CO poisoning. Then there is the interface site, which appears to be less prone to CO poisoning due to electronic interactions. A difference in reactivity between these interface sites and metal sites may exist, as shown by the differences in the activation energy and turnover rate of the ethylene hydrogenation reaction with CO on both model catalyst systems. The difference could also be the result of the relative mobilities of species on the surface. Scanning tunneling microscopy (STM) results from earlier work in our group have shown that ordered structures appear for the ethylene hydrogenation reaction over Rh(111) single crystal catalysts when CO molecules are introduced into the system [29]. The adsorption of CO on vacant hollow sites prevents the diffusion of ethylidyne. Because the surface becomes full of these immobile adsorbates, the ethylene from the gas phase has no room to adsorb and hydrogenation is prevented. Mobility is necessary to free up active hydrogenation sites. It is possible that the CO molecule retains its mobility at the oxide–metal interface sites on the Pt nanoparticle array model catalyst, which would keep these sites catalytically active for hydrogenation. The Pt nanoparticle array also has an alumina support, which can play a factor in diffusion and spillover effects of CO. The support material will be changed to other oxides, such as silica or titania, to determine the effects of the support. CO could induce a reconstruction of the Pt nanoparticle surface, creating domain boundaries, which would then increase CO diffusion. The Pt nanoparticle arrays could also be exposing a different crystalline face at the interface that is not prone to CO poisoning, thus allowing the reaction chemistry to take place at another type of site. The strength of the adsorption of the CO molecule on the catalyst surface must be further investigated. ΔH_{ads} is related to the mobility of the molecule on the catalyst surface, with weakly bound species enjoying greater mobility. The residence time of CO at these interfacial sites is small if the molecule is very mobile, and this would keep the sites available for reaction. More studies are necessary to gain an understanding of the differences in reaction mechanism for CO poisoning of the ethylene hydrogenation reaction over Pt(111) single crystal and Pt nanoparticle array model catalysts.

4. Conclusions

CO poisoning of the ethylene hydrogenation reaction has been studied on Pt(111) and Pt nanoparticle array model catalysts. Rate studies for Pt(111) show that the reaction is poisoned by CO, with the activation energy increasing from 10.8 to 20.2 kcal/mol. This poisoned activation energy is near the desorption energy of CO. Rate measurements for the CO-poisoned ethylene hydrogenation over the Pt nanoparticle arrays show a decrease in activity, but not a meaningful increase in activation energy. The activation energies for the ethylene hydrogenation reaction over the Pt nanoparticles with and without CO are 11.4 and 10.2 kcal/mol, respectively. The oxide–metal interface sites might therefore remain active for ethylene hydrogenation, which in turn suggests these sites remain free of adsorbed CO.

Acknowledgment

This work was supported by the Director, Office of Energy Research, Office of Basic Energy Sciences, Material Sciences Division, of the US Department of Energy under contract No. DE-AC03-76F00098.

References

[1] G.C. Bond, Acc. Chem. Res. 26 (1993) 490.
[2] G.A. Somorjai, *Introduction to Surface Chemistry and Catalysis* (Wiley, New York, 1994), Chapter 7.
[3] M. Arai, J. Chem. Eng. Jpn. 30 (1997) 1123.
[4] M. Valden, S. Pak, X. Lai and D.W. Goodman, Catal. Lett. 56 (1998) 7.
[5] S.L. Kiperman, React. Kinet. Catal. Lett. 68 (1999) 165.
[6] G.H Vurens, M. Salmeron, and G.A. Somorjai, Prog. Surf. Sci. 32 (1989) 333.
[7] P.R. Watson and G.A. Somorjai, J. Catal. 72 (1981) 347.
[8] K. Hayek, M. Fuchs, B. Klotzer, W. Reichl and G. Rupprechter, Top. Catal. 13 (2000) 55.
[9] K. Hayek, R. Kramer and Z. Paal, Appl. Catal. A: Gen. 162 (2000) 55.
[10] W.C. Conner and J.L. Falconer, Chem. Rev. 95 (1995) 759.
[11] M. Boudart, Adv. Catal. 20 (1969) 153.
[12] Z. Paal and G.A. Somorjai, in: *Handbook of Heterogeneous Catalysis*, eds. G. Ertl, H. Knozinger and J. Weikamp (Wiley-VCH, Weinheim, 1998).
[13] B.E. Hayden and A.M. Bradshaw, Surf. Sci. 125 (1983) 787.
[14] M. Trenary, K.J. Uran and J.T. Yates, Surf. Sci. 157 (1985) 512.
[15] W.K. Kuhn, J. Szanyi and D.W. Goodman, Surf. Sci. 274 (1992) L611.
[16] P. Hollins and J. Pritchard, Prog. Surf. Sci. 19 (1985) 275.
[17] M. Tushaus, E. Schweizer, P. Hollins and A.M. Bradshaw, J. Electron Spectrosc. Relat. Phenom. 44 (1987) 305.
[18] A. Crossley and D.A. King, Surf. Sci. 68 (1977) 528.
[19] J.W. Niemantsverdriet, *Spectroscopy in Catalysis: an Introduction* (Wiley-VCH, Weinheim, 2000).
[20] K.Y. Kung, P. Chen, F. Wei, G. Rupprechter, Y.R. Shen and G.A. Somorjai, Rev. Sci. Instrum. 72 (2001) 1806.
[21] P. Chen, S. Wasterberg, K.Y. Kung, J. Zhu, J. Grunes and G.A. Somorjai, Appl. Catal. A Gen. 229 (2002) 147.
[22] A.S. Eppler, J. Zhu, E.A. Anderson and G.A. Somorjai, Top. Catal. 13 (2000) 33.

[23] J. Zhu and G.A. Somorjai, Nano Lett. 1 (2001) 8.
[24] J. Grunes, J. Zhu, E.A. Anderson and G.A. Somorjai, J. Phys. Chem. B 106 (2002) 11463.
[25] F. Zaera and G.A. Somorjai, J. Am. Chem. Soc. 106 (1984) 2288.
[26] J.A. Jensen, K.B. Rider, M. Salmeron and G.A. Somorjai, Phys. Rev. Lett. 80 (1998) 1228.
[27] Y.Y. Yeo, L. Vattuone and D.A. King, J. Chem. Phys. 106 (1997) 392.
[28] M.E. Levin, M. Salmeron, A.T. Bell and G.A. Somorjai, J. Catal. 106 (1987) 401.
[29] K.S. Hwang, M. Yang, J. Zhu, J. Grunes and G.A. Somorjai, J. Mol. Catal. A (submitted for publication).